OFFICE OF NAVAL RESEARCH

Contract N00014-82K-0612

Task No. NR 627-838

TECHNICAL REPORT NO. 42

Luminescence Probe Studies of Ionomers. 3. Distribution of Decay Rate Constants for Tris Bipyridyl Ruthenium(II) in Nafion Membranes

by

Jorge L. Colón and Charles R. Martin*

Prepared for publication

in

The Journal of Physical Chemistry

Department of Chemistry
Texas A&M University
College Station, TX 77843

December 2, 1989

UNCLASSIFIED
SECURITY CLASSIFICATION OF THIS PAGE

REPORT DOCUMENTATION PAGE

Form Approved
OMB No 0704-0188

1a REPORT SECURITY CLASSIFICATION UNCLASSIFIED	1b. RESTRICTIVE MARKINGS
2a. SECURITY CLASSIFICATION AUTHORITY	3. DISTRIBUTION/AVAILABILITY OF REPORT APPROVED FOR PUBLIC DISTRIBUTION,
2b. DECLASSIFICATION/DOWNGRADING SCHEDULE	DISTRIBUTION UNLIMITED.
4. PERFORMING ORGANIZATION REPORT NUMBER(S) ONR TECHNICAL REPORT # 42	5. MONITORING ORGANIZATION REPORT NUMBER(S)
6a. NAME OF PERFORMING ORGANIZATION Dr. Charles R. Martin Department of Chemistry 6b. OFFICE SYMBOL (If applicable)	7a. NAME OF MONITORING ORGANIZATION Office of Naval Research
6c. ADDRESS (City, State, and ZIP Code) Texas A&M University College Station, TX 77843-3255	7b. ADDRESS (City, State, and ZIP Code) 800 North Quincy Street Arlington, VA 22217
8a. NAME OF FUNDING/SPONSORING ORGANIZATION Office of Naval Research 8b. OFFICE SYMBOL (If applicable)	9. PROCUREMENT INSTRUMENT IDENTIFICATION NUMBER Contract # N00014-82K-0612
8c. ADDRESS (City, State, and ZIP Code) 800 North Quincy Street Arlington, VA 22217	10. SOURCE OF FUNDING NUMBERS PROGRAM ELEMENT NO. / PROJECT NO. / TASK NO / WORK UNIT ACCESSION NO
11. TITLE (Include Security Classification)	
12. PERSONAL AUTHOR(S) Jorge L. Colon and Charles R. Martin	
13a. TYPE OF REPORT Technical 13b. TIME COVERED FROM _____ TO _____	14. DATE OF REPORT (Year, Month, Day) (89,12,02) Dec. 2, 1989 15. PAGE COUNT
16. SUPPLEMENTARY NOTATION Luminescence Probe Studies of Ionomers. 3. Distribution of Decay Rate Constants for Tris Bipyridyl Ruthenium(II) in Nafion Membranes	
17. COSATI CODES FIELD / GROUP / SUB-GROUP	18. SUBJECT TERMS (Continue on reverse if necessary and identify by block number) $Ru(bpy)_3^{2+}$, Nafion, heterogeneity $-SO_3H$, Nafion membrane Probe ions, decay kinetics.

19. ABSTRACT (Continue on reverse if necessary and identify by block number)

Measurements of the luminescence lifetime of $Ru(bpy)_3^{2+}$ (bpy = 2,2'-bipyridine) in Nafion were used to probe the heterogeneity of $-SO_3H$ sites in the Nafion membrane. The decay kinetics of the probe ion are shown to depart from simple first-order behavior. Albery's model of a continuous distribution of rate constants is used to explain the decay kinetics. The results of these and related investigations indicate that the probe ions reside in sites with different local water activities.

20. DISTRIBUTION/AVAILABILITY OF ABSTRACT ☒ UNCLASSIFIED/UNLIMITED ☐ SAME AS RPT ☐ DTIC USERS	21. ABSTRACT SECURITY CLASSIFICATION UNCLASSIFIED
22a NAME OF RESPONSIBLE INDIVIDUAL Dr. Robert Nowak	22b. TELEPHONE (Include Area Code) (202) 696-4410 22c. OFFICE SYMBOL

DD Form 1473, JUN 86 *Previous editions are obsolete.* SECURITY CLASSIFICATION OF THIS PAGE

UNCLASSIFIED

LUMINESCENCE PROBE STUDIES of IONOMERS. 3. DISTRIBUTION OF DECAY RATE CONSTANTS for TRIS BIPYRIDYL RUTHENIUM(II) in NAFION MEMBRANES

Jorge L. Colón and Charles R. Martin*

Department of Chemistry

Texas A&M University

College Station, Texas 77843

* To whom correspondence should be addressed.

Abstract

Measurements of the luminescence lifetime of $Ru(bpy)_3^{2+}$ (bpy = 2,2'-bipyridine) in Nafion were used to probe the heterogeneity of $-SO_3H$ sites in the Nafion membrane. The decay kinetics of the probe ion are shown to depart from simple first-order behavior. Albery's model of a continuous distribution of rate constants is used to explain the decay kinetics. The results of these and related investigations indicate that the probe ions reside in sites with different local water activities.

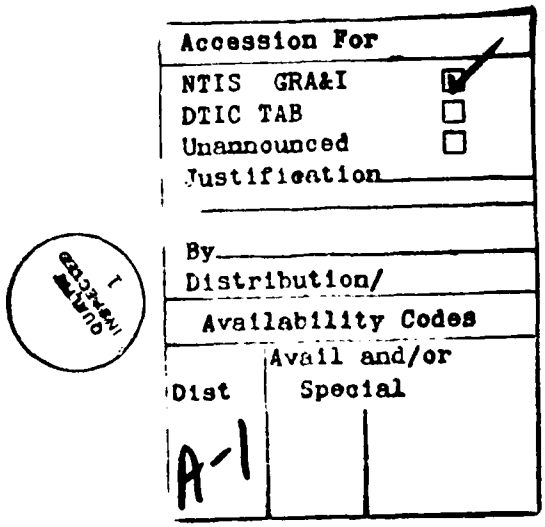

Introduction

Ion-containing polymers (ionomers) have a wide variety of applications including uses in electrochemistry, chemical synthesis, and separation science.[1-13] Nafion, a family of perfluorosulfonate ionomers marketed by Du Pont, has proven to be an extremely useful and versatile ion-containing polymer. Nafion and other ionomers have an unusual morphology in which the charged groups aggregate to form domains called ionic clusters. These clusters resemble reversed micelles and are randomly distributed throughout the backbone chain material phase.[14,15] The precise details of this structure are still unknown.

Information on the structural and dynamic nature of Nafion is a prerequisite for the future utilization of this material. Specifically, information about the chemical microenvironment and diffusion of ions and molecules within the ionic clusters is required. Luminescence probe techniques can provide photophysical and photochemical information about the properties of this system. For this reason, we and others[16-27] have been using luminescence probe techniques to study the morphology and chemical characteristics of the ionic cluster phases in ionomers.

The specific luminescent probe molecule used in this study is tris(2,2'-bipyridyl) ruthenium(II), $Ru(bpy)_3^{2+}$, an extensively studied metal complex.[28-30] Lee and Meisel reported luminescence quenching studies of $Ru(bpy)_3^{2+}$ in Nafion.[16] Lee and Meisel observed that the luminescence decay of $Ru(bpy)_3^{2+}$ in Nafion was monoexponential; in contrast, we have always obtained

nonexponential decays for the luminescence of $Ru(bpy)_3^{2+}$ in Nafion. Possible reasons for the discrepancies between our results and those of Lee and Meisel will be presented here.

The nonexponential luminescence decay curves reported in this paper can be fitted using a biexponential decay model. However, by fitting the data to this model it is tacitly assumed that $Ru(bpy)_3^{2+}$ exists in two distinct chemical environments within the Nafion membrane. An alternative to fitting the data to the biexponential model is to assume that a continuous distribution of chemical microenvironments exists within the membrane. This distribution of microenvironments produces a continuous distribution of luminescence decay rate constants.

We have used Albery's model for dispersed kinetics to analyze the luminescence of $Ru(bpy)_3^{2+}$ in Nafion membrane.[31] The fits of the experimental data to the dispersed kinetics model are better than the fits to the biexponential decay model. This data analysis shows that the decay of $Ru(bpy)_3^{2+}$ in Nafion can be described by a Gaussian distribution of the energy of activation for the decay. Information about the chemical distribution and nature of the ion exchange sites in the polymer phase can be obtained from this analysis. These and related results are presented in this paper.

Experimental Section

MATERIALS. Nafion 117 membrane (proton form) was obtained from the E.I. Du Pont Company. $Ru(bpy)_3Cl_2 \cdot 6H_2O$ was obtained from G. F. Smith and was used as received. Water was circulated through

a Milli-Q water purification system (Millipore Corp.) or was pyrolytically triply distilled. All other reagents and solvents were of the highest available grade and were used without further purification. All glassware was cleaned in 2M HNO_3 which had been doubled distilled in quartz (Seastart).

PROCEDURES. As-received Nafion membrane was cut into ca. 10 X 30 mm rectangles. The precut membranes were then cleaned by ultrasonicating in several portions of pyrolytically triply distilled water (PTD-H_2O), and then ultrasonicating in 50:50 EtOH-PTD-H_2O (0.5 hr.). The membranes were then boiled in PTD-H_2O for 2 hr. and rinsed ultrasonically in PTD-H_2O. The membranes were changed to the Na^+ form by soaking overnight in 1M NaOH, and finally rinsed ultrasonically in PTD-H_2O.

The wet membranes were weighed separately and placed in glass vials. Two of the membranes were used to determine the equilibrium membrane water content. These two membranes were dried in a vacuum oven overnight at 115°C and reweighed. The water content was calculated as percent by weight (100 X (weight of H_2O) / (weight of dry polymer)).

The luminescent probe $Ru(bpy)_3^{2+}$ was incorporated (loaded) into the remaining Nafion membranes by stirring each membrane in a separate vial containing the required concentration of $Ru(bpy)_3^{2+}$. (The aqueous solution of $Ru(bpy)_3^{2+}$ used to load $Ru(bpy)_3^{2+}$ into the membranes is called the "loading solution"; each membranes was placed in a loading solution containing the precise concentration of $Ru(bpy)_3^{2+}$ needed to load the membrane to

the desired $Ru(bpy)_3^{2+}$ level.) As will be discussed in detail later, because diffusion of the probe into the polymer phase is slow, the membranes were equilibrated with their respective loading solution for 1 month before use. The quantity of $Ru(bpy)_3^{2+}$ loaded was maintained very low; between 0.8 and 0.01% of the ionic sites in the Nafion membranes were exchanged with the luminescent probe. After loading, and previous to measurement, the membranes were rinsed with water.

Some experiments were performed on oxygen-free Nafion membranes. Oxygen was removed from the Nafion membranes as follows: After loading with $Ru(bpy)_3^{2+}$ the membrane was placed in a 12.5 mm X 12.5 mm X 45 mm rectangular cuvette filled with water. The cuvette was sealed with a rubber septum, and nitrogen was bubbled into the solution for one and a half hours while the solution was ultrasonicated.

SPECTROSCOPY. Steady-state emission spectra were obtained with a Spex Fluorolog 2 spectrofluorometer. The samples were excited with a 450-W xenon lamp and all the slits were set at 1.25 mm. The excitation wavelenght was 452 nm. Luminescence was detected perpendicular to the incident radiation. Luminescence lifetime measurements were obtained using a time-correlated single photon counting spectrometer (Edinburgh Instruments Model 199). The spectrometer is fitted with a nitrogen flashlamp (337 nm) and a microcomputer (IBM PS/2 Model 30 with a 8087 microprocessor).

The $Ru(bpy)_3^{2+}$-loaded membranes were sandwiched between two quartz slides. This assembly was positioned in the spectrometer

at 45 degrees to the axis of excitation. Emission was detected from the opposite side of the membrane at 45 degrees to the axis of the detector. This orientation (and the emission filter) minimizes the detection of scattering from the membranes.

Data Analyses. The general approach for obtaining kinetic parameters from the luminescence decay curves was described previously.[32] We fitted the experimental intensity vs. time transients to specific decay models using the method of nonlinear least-squares[33,34] (Marquardt algorithm); the Edinburgh Instrument's or MTR Software Inc.'s nonlinear least-squares software was used. The Marquardt algorithm minimizes the goodness-of-fit parameter chi square (χ^2) given by

$$\chi^2 = \Sigma \{ (1/\sigma_i^2) [y_i - y(t_i)]^2 \} \quad (1)$$

where σ_i are the uncertainties (errors) in the data points y_i and $y(t_i)$ is the value of the fitting function at each data point. For single photon counting data $\sigma_i^2 = y_i$.[33,34]

Three different decay models were used to fit the decay curves. The first two models were either a monoexponential or a biexponential decay model.[33] These models assume that one or two populations of emitters exist in the system.

The third model used to fit our data is Albery's dispersed kinetics model, which takes into account the heterogeneous nature of the system. The luminescence of molecules emitting from heterogeneous systems (e.g, proteins, surfaces, and micelles)

frequently depart from first-order kinetics.[35] Therefore, a plot of the logarithm of emission intensity vs. time is nonlinear. Albery's model accounts for this departion from first-order kinetics.

Albery's model is an adaptation of a new model for interpreting the decay kinetics in nonhomogeneous systems.[31,36-48] Rather than assuming just one or two distinct populations of emitters, this model assumes that a continuous distribution of decay rates exits within the heterogeneous system. This continuous distribution of decay rates results from a continuous distribution of chemical microenvironments within the system; each microenvironment has a distinct decay rate constant. This model assumes that each of these distinct rate constants is first-order.

Recently, Albery et al.[31] proposed this general model for dispersed kinetics in heterogeneous systems. This model assumes that the dispersion in the kinetics is the result of a change in energy of activation for the reaction at different sites in the system. Albery's model assumes that the observed kinetics can be described by a Gaussian distribution of the energies of activation, or of the natural logarithm of the decay rate constant.

We have used Albery's model as the third approach for fitting our experimental emission decay curves. The equation used to fit the decay curves to this Gaussian distribution model is:[31]

$$C/C_o = \frac{\int_{-\infty}^{+\infty} \exp(-x^2)\ \exp[-\tau\ \exp(\gamma x)]\ dx}{\int_{-\infty}^{+\infty} \exp(-x^2)\ dx} \qquad (2)$$

where $$\int_{-\infty}^{+\infty} \exp(-x^2)\ dx = \pi^{1/2}$$

C is the concentration of excited state species at any time, t, after excitation, C_o is the excited state concentration at t = 0, x is the parameter that describes the Gaussian (see Appendix), γ corresponds to the width of the distribution, and $\tau = \bar{k}t$. The decay rate constant of maximum probability is $\bar{k}$. The τ in Equation 4 should not be confused with the average lifetime for the emitter which is $1/\bar{k}$. The integral in Equation 2 is solved numerically as described by Albery et al.[31] Equation 2 is derived in the Appendix.

Albery's dispersed kinetics model provides the "most probable" rate constant, $\bar{k}$, which is the first-order rate constant associated with the average chemical microenvironment within the medium. This rate constant can be studied in the normal fashion as if the process was exponential (i.e., normal kinetic analysis can be performed with this "most probable" rate constant value). The dispersion of k (the γ value) provides a measure of the disorder of the medium. This information can be used to investigate the local structure of the medium and the dependence of the rate process on energetic and structural parameters.[48]

Results and Discussion

Previous Investigation of $Ru(bpy)_3^{2+}$ Emission from Nafion. Lee and Meisel[16] observed monoexponential decay curves for the emission of $Ru(bpy)_3^{2+}$ in Nafion. We have repeated this experiment numerous times over the last 5 years and have never observed monoexponential decays. Recently, Kaneko and Hayakawa[49] also observed that the decay of $Ru(bpy)_3^{2+}$ in Nafion films cannot be describe by a monoexponential decay model. Figure 1 shows typical decay curves for $Ru(bpy)_3^{2+}$ in Nafion at various loading levels; note that these are semilogarithmic plots. The nonlinearity observed in Figure 1 clearly shows that a monoexponential decay model is not appropriate.[33] Nonlinear semilogarithmic plots such as these have been observed consistently by our group, independent of instrument, operator, or time.

We believe that it is possible that Lee and Meisel's results were affected by a nonequilibrium distribution of luminescent probe ions in the Nafion membrane. Lee and Meisel stirred their membranes in the $Ru(bpy)_3^{2+}$ loading solution for only 12 hours. A simple calculation shows that equilibrium times well in excess of 12 hours are required if probe-membrane equilibrium is to be achieved. The distance, Δ, a diffusing species moves in time, t, is given by $\Delta = (2Dt)^{1/2}$ where D is the diffusion coefficient.[50] Assuming D for $Ru(bpy)_3^{2+}$ in Nafion is 2×10^{-10} cm^2/s,[7] a $Ru(bpy)_3^{2+}$ ion moves, on average, only 0.004 cm into a Nafion membrane during a 12 hour equilibrium period. In

order to achieve equilibrium the ion must move half-way through the membrane (0.0125 cm). Thus, after 12 hours, a nonhomogeneous distribution of $Ru(bpy)_3^{2+}$ is extant in the membrane; electron microprobe analyses have experimentally confirmed such nonhomogeneous distributions.[51]

It is not obvious why an nonhomogeneous distribution of $Ru(bpy)_3^{2+}$ in the membrane would yield a monoexponential decay. We have found, however, that after loading, the wavelength of maximum emission intensity for $Ru(bpy)_3^{2+}$ blueshifts for periods of up to one month. This blue shift results from a gradual partitioning of the probe from domains with high local water activity to domains with high local fluorocarbon chain material activity (vide infra and ref. 19). These data suggest that $Ru(bpy)_3^{2+}$, in freshly-loaded films, is predominately present in an aqueous-like environment. Since only this aqueous-like environment is populated at short equilibration times, a monoexponential decay (as observed by Lee and Meisel) might be anticipated. In contrast, for long equilibration periods a variety of microenvironments become populated (aqueous-like and fluorocarbon-like) and this produces the nonexponential decay observed in our experiments.

Biexponential Decay Model. The biexponential decay model assumes that there are two distinct populations of emitters (or two distinct chemical microenvironments) within the membrane phase. As a result of these populations, two distinct decay rate constant or decay lifetimes are observed. Figure 1 shows that

our data can be fitted to a biexponential decay model. The lifetimes, standard deviations, and χ^2 values obtained from these fits are shown in Table I.

The kinetic data obtained from the biexponential decay model (Table I) may be summarized as follows. At loading levels less than 0.07%, both the long and the fast lifetimes increase with the quantity of $Ru(bpy)_3^{2+}$ loaded into the membrane. Furthermore, the data in Table I suggest that the microenvironment yielding the long lived species is preferentially occupied. (At low loading levels 84 to 98% of the emitters occupy sites in this microenvironment, while at higher loading levels, only 68 to 84% of the emitters are in this long lifetime environment.) Above 0.07% loading, the lifetimes and relative sizes of the two populations remain more or less constant (Table I). Kaneko and Hayakawa[49] described the decay of $Ru(bpy)_3^{2+}$ adsorbed in Nafion at a low loding level as a biexponential decay with long lifetime component of 750-839 ns (over 90%) and a fast lifetime component of 121-238 ns.

The kinetic data in Table I suggest that the biexponential decay model is not appropriate for this system. The first problem with this model concerns the changes in both the short and long lifetimes, observed at low loading levels. If two distinct populations exist in the membrane, the two lifetimes obtained from the kinetic analysis should be the same regardless of the loading level; the relative numbers of emitters in each population might change with loading, but there is no a priori

reason to expect that the lifetime will. The change in lifetimes observed in Table I suggest that more than two distinct environments are being populated.

The data obtained from the biexponential model also contradicts evidence obtained from steady-state emission experiments. Table II shows that the wavelength of maximum emission intensity (λ_{max}) is strongly blue shifted (relative to emission from water) at low loading levels; λ_{max} shifts to more aqueous-like values at higher loading levels. The blue-shifted λ_{max} clearly shows that the first $Ru(bpy)_3^{2+}$ ions which enter the membrane occupy sites with high local fluorocarbon chain material activity (and low local water activity).[52] When these sites are occupied the subsequently-loaded $Ru(bpy)_3^{2+}$'s enter sites with higher local water activities; this produces the shift in λ_{max} to more aqueous-like (and less fluorocarbon-like[52]) values.

While the lifetime data obtained from the biexponential decay model (Table I) show evidence for preferential occupancy of one environment over the other, the lifetimes are reversed. Note that the results from the biexponential model (Table I) suggest that at low loading the long (aqueous-like) lifetime is preferentially occupied (Table I). This is in direct contradiction to the steady-state data which suggest that the nonaqueous or fluorocarbon-like environment is preferentially occupied (Table II).

The final problem with the biexponential decay model data concerns the very short lifetime observed at low loading levels.

It is difficult to explain how such a low lifetime for $Ru(bpy)_3^{2+}$ could be physically achieved; for example, while $Ru(bpy)_3^{2+}$'s emission parameters from numerous solvents have been investigated,[28] none of these solvents yield such short lifetimes. One possible explanation, which will be explored in detail below, is that the lifetime, at low loading, is decreased by O_2 quenching. However, the concentration of O_2 in the membrane[53] is too low to yield such dramatically reduced lifetimes.

The bottom line is that, while it is impossible to state with 100% assurance that a model is, or is not, appropriate for a particular system, the bulk of the evidence suggests that the biexponential decay model is not appropriate here. Furthermore, as will be shown below, the dispersed kinetics model provides statistically better fits to the experimental data.

Dispersed Kinetics Model. The data in Tables I and II suggest that more than two chemical microenvironments are present in Nafion membrane; this has been confirmed by Mossbauer investigations of Fe^{3+}-exchanged Nafion[54,55] and infrared and NMR studies of water in Nafion membranes.[56,57] Faulkner and Bartolo have recently proposed that a continuous distribution of chemical microenvironments exists, for $Ru(bpy)_3^{2+}$, within the cation exchange polymer poly(styrenesulfonate) (PSS).[58] These authors used the dispersed kinetics model of Albery et al.[31] to analyze $Ru(bpy)_3^{2+}$ emission data for PSS.

Figure 2 shows that Albery's dispersed kinetics model can be fitted to the experimental $Ru(bpy)_3^{2+}$ decay data obtained here. Two independently adjustable parameters k, the average decay rate constant and γ, the width of the distribution, were used to obtain these fits. These kinetic parameters, as well as the χ^2 values for the fits, are shown in Table III.

The χ^2 values obtained using the dispersed kinetics model (Table III) are essentially identical, at all loading levels, to the χ^2 values obtained from the biexponential model (Table I). This would seem to suggest that neither model is preferable; however, four independently adjustable parameters (Two k's and two B's) were used in the biexponential fit, whereas only two adjustable parameters were used for the dispersed kinetics model. Thus, in addition to the arguments presented above, the principle of "Ockham's Razor"[59] makes the dispersed kinetics model preferable to the biexponential model. More important than the philosophical "Ockham's Razor" argument, the standard deviation for the parameters obtained from the fit to the dispersed kinetics model were always smaller than for the biexponential fit (Table I and III). This provides quantitative statistical evidence that the dispersed kinetics model provides a better fit to the experimental data.

Albery's dispersed kinetics model is a functional mathematical model that can be used to obtain kinetic information. How can this information be translated into a chemical model? A chemical picture can be envisioned in which

the clusters of Nafion offer a variety of chemical microenvironments to the $Ru(bpy)_3^{2+}$ ions. These microenvironments arise because different parts of the clusters have different dielectric constants, depending on the amount of water and perfluorocarbon chain material present.

The characteristics of a specific chemical microenvironment can have a significant impact on the $Ru(bpy)_3^{2+}$ decay rate. The lifetiem of $Ru(bpy)_3^{2+}$'s metal-to-ligand charge transfer (MLCT) excited-state decay is dependent on both radiative and nonradiative modes of deactivation.[28-30] In addition, the excited-state decay is dependent on thermal activation to, and subsequent decay from, low-lying dd states. These processes are known to be dependent on the chemical microenvironment in which $Ru(bpy)_3^{2+}$ resides.[28-30] Thus, the excited-state lifetime will vary from microenvironment to microenvironment within the membrane.

Recent studies have demonstrated the effects of the properties of the chemical microenvironment on the emission characteristics of $Ru(bpy)_3^{2+}$. Meyer et al.[60] have observed nonexponential decays for a Ru(II) polypyridyl complex bound to a chlorosulfonated polystyrene film. The observed lifetimes were dependent on the hydrophobicity and structure of the chemical sites within the film. Furthermore, Vining and Meyer[61] have presented electrochemical and spectroelectrochemical evidence for at least three different chemical regions within Nafion films. The presence of oxygen in these regions brings another decay mechanism for the deactivation of $^*Ru(bpy)_3^{2+}$.

The k values obtained from the fits to the dispersed kinetic model can be used to calculate the mean lifetime, τ, values for each $Ru(bpy)_3^{2+}$ loading level. These τ values are shown in Table III. The τ value for the lowest loading level appears to be significantly lower than the other τ's. Applying the standard Q test for rejection of data,[62] we find that at the 99% confidence level, the τ associated with the lowest loading level is significantly less than the τ's obtained at the high loading levels. Furthermore, the average τ value obtained from the higher (0.03 to 0.80%) loading levels (435 ± 8 ns) is identical to the lifetime for $Ru(bpy)_3^{2+}$ in aerated aqueous solution (434 ns).

The trends in the kinetic parameters obtained from the dispersed kinetics model (Table III) agree, phenomenologically, with the trends in the steady-state emission data (Table II). Both data show that an aqueous-like environment is populated at high loading levels whereas a "non-aqueous" environment is preferentially populated at low loading levels. As noted above, this "non-aqueous" environment simply means that the first $Ru(bpy)_3^{2+}$'s which enter the membrane preferentially occupy sites with high local fluorocarbon chain material activities and low water activities; given the known hydrophobicity of $Ru(bpy)_3^{2+}$, this preference for hydrophobic sites is not surprising.[52]

The width of the distribution (γ values in Table III) also follow the trends observed in the τ and λ_{max} values; as the loading level is increased the overall Gaussian distribution is

reduced in width. This reduction in width occurs because many of the component lifetimes are similar in the aqueous-like domains and because a relatively smaller number of the fast-decaying species are present. Therefore, at higher loading levels there is a smaller contribution of the ions in the "non-aqueous" sites to the total distribution.

The question which arises, however, is why would a high local chain material-activity microenvironment yield a diminished lifetime for $Ru(bpy)_3^{2+}$. We believe that part of this diminution in $Ru(bpy)_3^{2+}$ lifetime results from a higher local O_2 activity. It is well known that O_2 is more soluble in fluorocarbon-containing media than in pure water.[53,63] For example, Lee and Rodgers[63] have shown that singlet oxygen is five times more soluble in the perfluorocarbon region than in the water clusters. Thus, we propose that the "non-aqueous" sites are also sites of high local O_2 activity. Thus, the $Ru(bpy)_3^{2+}$'s which occupy these high fluorocarbon chain material-activity sites have shorter lifetimes due to the higher local quencher concentrations.

The effect of the local O_2 activity on the lifetime of $Ru(bpy)_3^{2+}$ was confirmed by performing luminescence lifetimes studies of $Ru(bpy)_3^{2+}$ in Nafion membranes that have been deaerated (oxygen removed). Figure 3 compares two luminescence decay curves for the same loading level of $Ru(bpy)_3^{2+}$ in aerated and deaerated Nafion membranes. Figure 3 clearly shows that the luminescence decay for the deaerated membrane is longer lived than the luminescence decay in the aerated membrane.

Table IV shows the kinetic parameters obtained from the fit of the luminescence decay curves from the deaerated membranes to the dispersed kinetics model. In agreement with the data in Figure 3, the lifetimes for the deaerated membranes are longer than the corresponding lifetimes in the aerated membranes. This observation confirms that oxygen quenches the luminescence of $Ru(bpy)_3^{2+}$ in the aerated membranes.

The kinetic parameters for the deaerated membranes (Table IV) show the same trends as the kinetic parameters for the aerated membranes (Table III). The $Ru(bpy)_3^{2+}$ luminescence lifetime increases at higher loading levels for both the deaerated and aerated membranes. The increase in luminescence lifetime indicates that the later-loaded $Ru(bpy)_3^{2+}$ ions occupy different chemical microenvironments than the first-loaded metal ions. These results prove that a multiplicity of chemically distinct microenvironments exists in Nafion irrespectively of the presence of O_2. In addition, Table IV shows that the width of the distribution (γ value) is reduced as the $Ru(bpy)_3^{2+}$ loading increases in the deaerated membranes. As discussed for the aerated membranes, this reduction in the width of the distribution occurs because the relative number of fast decaying species is reduced at these high loading levels.

Previous studies[16,19] have suggested that $Ru(bpy)_3^{2+}$ preferentially resides at the interface between the water cluster and the perfluorocarbon backbone region. Furthermore, Lee and Meisel[21] observed that oxygen quenches the fluorescence of pyrene

in Nafion; pyrene also resides at, or near, the fluorocarbon/water cluster interphase.[19,21,27] The results presented here, and Lee and Meisel's results,[21] indicate that oxygen can access the water clusters in Nafion to quench the pyrene or the $Ru(bpy)_3^{2+}$ luminescence.

Finally, Table IV shows that, at high loading levels, the width of the distribution is smaller in deaerated membranes than in aerated membranes (Table III). The smaller width of the distribution occurs because the absence of O_2 reduces the number of chemically distinct sites in Nafion. This is in agreement with Lakowicz et al.[40] who proved that quenching causes a lifetime distribution to become wider and shift toward shorter decay times.

Conclusions

The dispersed kinetics model used here assumes a Gaussian distribution of the logarithm of the decay rate constant. However, other distribution models are possible (e.g., Lorentzian, which generally gives narrower distributions).[40] The distribution model used in the fitting equations could have also been a Gaussian or Lorentzian distribution of rate constants, or lifetimes, or energies of activation, etc. In addition, there is no reason to believe that the "real" lifetime distribution is symmetric. Finally, it is possible that a second distribution component should be included, making the distribution bimodal. At present there is no theoretical model to predict the exact distribution and therefore the selection of a particular

distribution model is made arbitrarily. However, the key question is whether the decay process is best described by discrete lifetimes or a continuous distribution of lifetimes; in the present case a distribution model is appropiate.

The results obtained here prove that oxygen is not the sole reason for the heterogeneity in the luminescence decay kinetics observed in Nafion. These results provide evidence for the existence of chemically distinct regions within Nafion which affect the lifetime of the excited state of $Ru(bpy)_3^{2+}$. As noted above, the radiative and nonradiative processes affecting the lifetime of $Ru(bpy)_3^{2+}$ are dependent on the medium in which $Ru(bpy)_3^{2+}$ resides.

The structural information gained in these studies can be related to the proposed models for the morphology of Nafion. For example, Gierke[64] developed a two-phase model (the cluster-network model) of the morphology of Nafion; according to this mode, the ionic clusters are spherical (ca. 40 Å in diameter) and are interconnected by narrow channels (ca. 10 Å in diameter). The cluster-network model assumes that both the ions and the solvent are localized within the clusters and channels.

Yeager and Steck[65] proposed a three-phase model where a region of fluorocarbon backbone material (with some microcrystallites) coexists with an ionic cluster region containing the majority of the $-SO_3^-$ sites, counter ions and sorbed water. An interface is presumed to exist between these two regions. This interface is an amorphous fluorocarbon region

containing pendant side chain material, some water, and some sulfonate sites with associated counterions. The clusters are no longer assumed to be spherical and intrusion of the fluorocarbon phase into the ionic clusters occurs. Our data support this interfacial model where there is a gradual transition between purely fluorocarbon and purely aqueous environments. It is this gradual transition which produces the continuous distribution of chemical microenvironments within the polymer phase.

These findings have some relevance to the electrochemical response of $Ru(bpy)_3^{2+}$ in Nafion. The results of this paper suggest that $Ru(bpy)_3^{2+}$ resides in a variety of distinct chemical microenvironments within Nafion membrane. The energetics of the redox reaction are clearly subject to the influence of these distinct microenvironments present in Nafion. For example, the redox waves can become broaded by the distribution of activation free energies for the redox reaction.[66] While broadening of the $Ru(bpy)_3^{2+}$ wave in Nafion is, indeed, observed, the chemical microenvironments are not so distinct as to produce distinct redox waves or shoulders.

Acknowledgements. Financial support for this work was provided by the Robert A. Welch Foundation, the Office of Naval Research, and the Air Force Office of Scientific Research. We gratefully acknowledge partial support of this research by the Regents of Texas A&M University through the AUF-sponsored Materials Science and Engineering Program. J.L.C. acknowledges support from the Texas A&M University Minority Merit Fellowship.

References

(1) Eisenberg, A., Yeager, H. L., Eds. Perfluorinated Ionomer Membranes; American Chemical Society: ACS, Washington, DC, 1982; ACS Symp. Ser. No. 180.

(2) Cutler, S. G. In Ions in Polymers, Eisenberg, A. Ed.; American Chemical Society: Washington, DC, 1980; Adv. Chem. Ser. No. 187, Chapter 9.

(3) White, H. S.; Leddy, J.; Bard, A. J. J. Am. Chem. Soc. 1982, 104, 4811.

(4) Martin, C. R.; Rubinstein, I.; Bard, A. J. J. Am. Chem. Soc. 1982, 104, 4817.

(5) Buttry, D. A.; Anson, F. C. J. Am. Chem. Soc. 1982, 104, 4824.

(6) Martin, C. R.; Rhoades, T. A.; Ferguson, J. A. Anal. Chem. 1982, 54, 1639.

(7) Martin, C. R.; Dollard, K. A. J. Electroanal. Chem. 1983, 159, 127.

(8) Buttry, D. A.; Saveant, J. M.; Anson, F. C. J. Phys. Chem. 1984, 88, 3086.

(9) Szentirmay, M. N.; Martin, C. R. Anal. Chem. 1984, 56, 1898.

(10) Moore, R. B. III; Wilkerson, J. E.; Martin, C. R. Anal. Chem. 1984, 56, 2572.

(11) Hsu, W. Y. In Coulombic Interactions in Macromolecular Systems, Eisenberg, A., Bailey, F. E., Eds.; American Chemical Society: ACS, Washington, DC, 1986; ACS Symp. Ser. No. 302, p. 120.

(12) Falk, M. In Structure and Properties of Ionomers, Pineri, M., Eisenberg, A., Eds.; D. Reidel Publishing Company: Dordrecht, 1987, pp. 141-148.

(13) Sonheimer, S. J.; Bunce, N. J.; Fyfe, C. A. JMS-Rev. Macromol. Chem. Phys. 1986, C26, 353.

(14) Gierke, T. D.; Munn, G. E.; Wilson, F. C. J. Polym. Phys. Ed. 1981, 19, 1687.

(15) Hsu, W. Y.; Gierke, T. D. Macromolecules 1982, 15, 101.

(16) Lee, P. C.; Meisel, D. J. Am. Chem. Soc. 1980, 102, 5477.

(17) Nagata, I.; Li, R.; Banks, E.; Okamoto, Y. Macromolecules 1983, 16, 903.

(18) Kuczynski, J. P.; Milosavljevic, B. H.; Thomas, J. K. J. Phys. Chem. 1984, 88, 980.

(19) Szentirmay, M. N.; Prieto, N. E.; Martin, C. R. J. Phys. Chem. 1985, 89, 3017.

(20) Szentirmay, M. N.; Prieto, N. E.; Martin, C. R. Talanta 1985, 32, 745.

(21) Lee, P. C.; Meisel, D. Photochem. Photobiol. 1985, 41, 21.

(22) Blatt, E.; Launikonis, A.; Mau, A. W.-H.; Sasse, W. H. F. Aust. J. Chem., 1987, 40, 1.

(23) Weir, D.; Scaiano, J. C. Tetrahedron 1987, 43, 1617.

(24) Wintgens, V.; Scaiano, J. C. Can. J. Chem. 1987, 65, 2131.

(25) Wong, E. K. L.; Richmond, G. L. Appl. Spectrosc. 1988, 42, 293.

(26) Niu, E.; Ghiggino, K. P.; Mau, A. W.-H.; Sasse, W. H. F. J. Luminesc. 1988, 40&41, 563.

(27) Blatt, E.; Sasse, W. H. F.; Mau, A. W.-H. J. Phys. Chem. 1988, 92, 4151.

(28) Kalyanasundaram, K. Coord. Chem. Rev. 1982, 46, 159.

(29) Seddon, E. A.; Seddon, K. R. The Chemistry of Ruthenium; Elsevier: Amsterdam, 1984, Chapter 15.

(30) Juris, A.; Balzani, V.; Barigelleti, F.; Campagna, S.; Belser, P.; Von Zelewsky, A. Coord. Chem. Rev. 1988, 84, 85.

(31) Albery, W. J.; Bartlett, P. N.; Wilde, C. P.; Darwent, J. R. J. Am. Chem. Soc. 1985, 107, 1854.

(32) Colón, J. L.; Yang, C.-Y.; Clearfield, A.; Martin, C. R. J. Phys. Chem. in press.

(33) O'Connor, D. V., Phillips, D. Time Correlated Single Photon Counting; Academic: London, 1984.

(34) Bevington, P. R. Data Reduction and Error Analysis in the Physical Sciences; McGraw Hill: New York, 1969.

(35) Thomas, J. K. Chemistry of Excitation at Interfaces; ACS Monograph 191; American Chemical Society: Washington, DC, 1983.

(36) James. D. R.; Ware, W. R. Chem. Phys. Lett. 1985, 120, 450, 455, 460.

(37) James, D. R.; Ware, W. R. Chem. Phys. Lett. 1986, 126, 7.

(38) James, D. R.; Turnbull, J. R.; Wagner, B. D.; Ware, W. R. Petersen, N. O. Biochemistry 1987, 26, 6272.

(39) Siemiarczuk, A.; Ware, W. R. J. Phys. Chem. 1987, 91, 3677.

(40) Lakowicz, J. R.; Cherek, H.; Gryczynski, I.; Joshi, N.; Johnson, M. L. Biophys. Chem. 1987, 28, 35.

(41) Lakowicz, J. R.; Johnson, M. L.; Wiczk, W.; Bhat, A.; Steiner, R. F. Chem. Phys. Lett. 1987, 138, 587.

(42) Gryczynski, I.; Wiczk, W.; Johnson, M. L.; Lakowicz, J. R. Chem. Phys. Lett. 1988, 145, 439.

(43) Gratton, E.; Barbieri, B. Spectroscopy 1986, 1, p.?.

(44) Alcala, J. R.; Gratton, E.; Prendergast, F. G.; Biophys. J. 1987, 51, 587.

(45) Alcala, J. R.; Gratton, E.; Prendergast, F. G.; Biophys. J. 1987, 51, 597.

(46) Alcala, J. R.; Gratton, E.; Prendergast, F. G.; Biophys. J. 1987, 51, 925.

(47) Parasassi, T.; Conti, F.; Gratton, E.; Sapora, O. Biochim. Biophys. Acta 1987, 898, 196.

(48) Siegbrand, W.; Wildman, T. Acc. Chem. Res. 1986, 19, 238.

(49) Kaneko, M.; Hayakawa, S. J. Macromol. Sci.-Chem. 1988, A25, 1255.

(50) Bockris, J. O'M.; Reddy, A. K. N. Modern Electrochemistry Plenum: New York, 1970.

(51) Kelly, J. M. In Structure and Properties of Ionomers, Pineri, M., Eisenberg, A., Eds.; D. Reidel Publishing Company: Dordrecht, 1987, pp. 127-140.

(52) Turro, N. J.; Lee, P. C. C. J. Phys. Chem. 1982, 86, 3367.

(53) Ogumi, Z.; Kuroe, T.; Takehara, Z. J. Electrochem. Soc. 1985, 132, 2601.

(54) Rodmacq, B.; Pineri, M.; Coey, J. M. D. Rev. Phys. Appl. 1980, 15, 1179.

(55) Rodmacq, B.; Pineri, M.; Coey, J. M. D.; Meagher, A. J. Polym. Sci., Polym. Phys. Ed. 1982, 20, 603.

(56) Kojima, J.; Kuwahara, N.; Kaneko, M. J. Chem. Phys. 1975, 63, 332.

(57) Boyle, N. G.; McBrierty, V. J.; Douglas, D. C. Macromolecules 1983, 16, 75.

(58) Faulkner, L. R.; Bartolo, R. G. Presented at the 194th Meeting of the American Chemical Society, New Orleans, August 30-September4, 1988, Paper ANYL 5.

(59) Webster's II New Riverside University Dictionary; The Riverside Publishing Company: Boston, 1984.

(60) Surridge, N. A.; McClanahan, S. F.; Hupp, J. T.; Danielson, E.; Gould, S.; Meyer, T. J. J. Phys. Chem. 1989, 93, 294.

(61) Vining, W. J.; Meyer, T. J. J. Electroanal. Chem. 1987, 237, 191.

(62) Skoog, D. A.; West, D. M. Fundamentals of Analytical Chemistry; 4th Edition; CBS College Publishing: Philadelphia, 1982.

(63) Lee, P. C.; Rodgers, M. A. J. J. Phys. Chem. 1984, 88, 4385.

(64) Gierke, T. D.; Hsu, W. Y. in Perfluorinated Ionomer Membranes, Eisenberg, A., Yeager, H. L., Eds.; American Chemical Society: Washington, DC, 1982; ACS Symp. Ser. No. 180, p.283.

(65) Yeager, H. L.; Steck, A. J. Electrochem. Soc. 1981, 128, 1880.

(66) Albery, W.J.; Boutelle, M. G.; Colby, P. J.; Hillman, A. R. J. Electroanal. Chem. 1982, 133, 135.

TABLE I. Kinetic and Statistical Parameters Obtained by Fitting a Biexponential Decay Model to the Experimental $Ru(bpy)_3^{2+}$ Emission Data.

$Ru(bpy)_3^{2+}$, %[a]	τ_{short} (%), ns[b]	τ_{long} (%), ns[b]	χ^2[c]
0.01	42.8 ± 11 (2.75)	442 ± 20 (97.25)	0.993
0.03	43.7 ± 13 (1.81)	475 ± 9 (98.19)	1.237
0.05	127 ± 48 (6.07)	505 ± 12 (93.93)	1.003
0.07	219 ± 53 (16.20)	613 ± 27 (83.80)	1.266
0.10	222 ± 42 (17.87)	633 ± 25 (82.13)	1.389
0.20	201 ± 24 (15.25)	606 ± 15 (84.75)	1.538
0.30	217 ± 27 (16.73)	608 ± 15 (83.27)	1.724
0.50	284 ± 26 (32.34)	758 ± 36 (67.66)	2.051
0.80	259 ± 24 (23.85)	657 ± 18 (76.15)	2.174

[a] Percent of $-SO_3^-$ sites in Nafion occupied by $Ru(bpy)_3^{2+}$.

[b] Error in lifetime value given as one standard deviation. Value in parenthesis is the percent of that lifetime component to the total luminescence decay.

[c] Reduced chi square value.

TABLE II. Dependence of Emission λ_{max} on the $Ru(bpy)_3^{2+}$ Loading Level in Nafion

$Ru(bpy)_3^{2+}$, % [a]	λ_{max}, nm
0.01	593
0.03	597
0.05	599
0.07	600
0.10	600
0.20	602
0.30	601
0.50	602
0.80	603

[a] Percent of $-SO_3^-$ sites in Nafion occupied by $Ru(bpy)_3^{2+}$.

TABLE III. Kinetic and Statistical Parameters Obtained by Fitting the Dispersed Kinetics Model to the Experimental $Ru(bpy)_3^{2+}$ Emission Data.

$Ru(bpy)_3^{2+}$, [a] %	$\bar{k} \times 10^6$, s^{-1}	τ, ns	γ	χ^2 [b]
0.01	2.639	379 ± 18	1.226	1.003
0.03	2.241	446 ± 8	0.842	1.204
0.05	2.365	423 ± 6	0.882	1.002
0.07	2.264	442 ± 5	0.826	1.262
0.10	2.292	436 ± 4	0.862	1.384
0.20	2.329	429 ± 3	0.894	1.538
0.30	2.306	434 ± 2	0.826	1.718
0.50	2.332	429 ± 2	0.740	2.066
0.80	2.278	439 ± 2	0.735	2.189

[a] Percent of $-SO_3^-$ sites in Nafion occupied by $Ru(bpy)_3^{2+}$.

[b] Reduced chi square value.

TABLE IV. Kinetic and Statistical Parameters Obtained by Fitting the Dispersed Kinetics Model to the Experimental $Ru(bpy)_3^{2+}$ Emission Data in Oxygen-Free Nafion Membranes.

$Ru(bpy)_3^{2+}$, %[a]	$\bar{k}$ X 10^6, s^{-1}	τ, ns	γ	χ^2[b]
0.01	1.726	579 ± 16	2.157	1.919
0.03	1.485	673 ± 6	0.919	3.208
0.05	1.361	735 ± 6	0.764	4.040
0.07	1.368	731 ± 6	0.868	4.208
0.10	1.372	729 ± 11	0.700	2.202
0.20	1.409	710 ± 7	0.619	2.728
0.30	1.377	726 ± 8	0.675	2.876
0.50	1.346	743 ± 7	0.633	3.371
0.80	1.324	755 ± 7	0.502	3.707

[a] Percent of $-SO_3^-$ sites in Nafion occupied by $Ru(bpy)_3^{2+}$.

[b] Reduced chi square value.

Figure 1. Points- Experimental luminescence decay data for $Ru(bpy)_3^{2+}$ from Nafion membrane. Loading levels were (A) 1 - 0.80%, 2 - 0.50%, 3 - 0.30%, 4 - 0.20%; (B) 1 - 0.10%, 2 - 0.07%, 3 - 0.05%, 4 - 0.03%. The solid curves are best fit curves obtained from the biexponential decay model.

Figure 2. Points - Experimental luminescence decay data for $Ru(bpy)_3^{2+}$ from Nafion membrane. Loading levels are (A) 0.80%, (B) 0.10%, (C) 0.03%. The solid curves are best fit curves obtained from the Albery's dispersed kinetics model.

Figure 3. (A) Luminescence decay curves for a deaerated $Ru(bpy)_3^{2+}$ exchanged Nafion membrane. (B) luminescence decay curve for an aerated Nafion membrane.

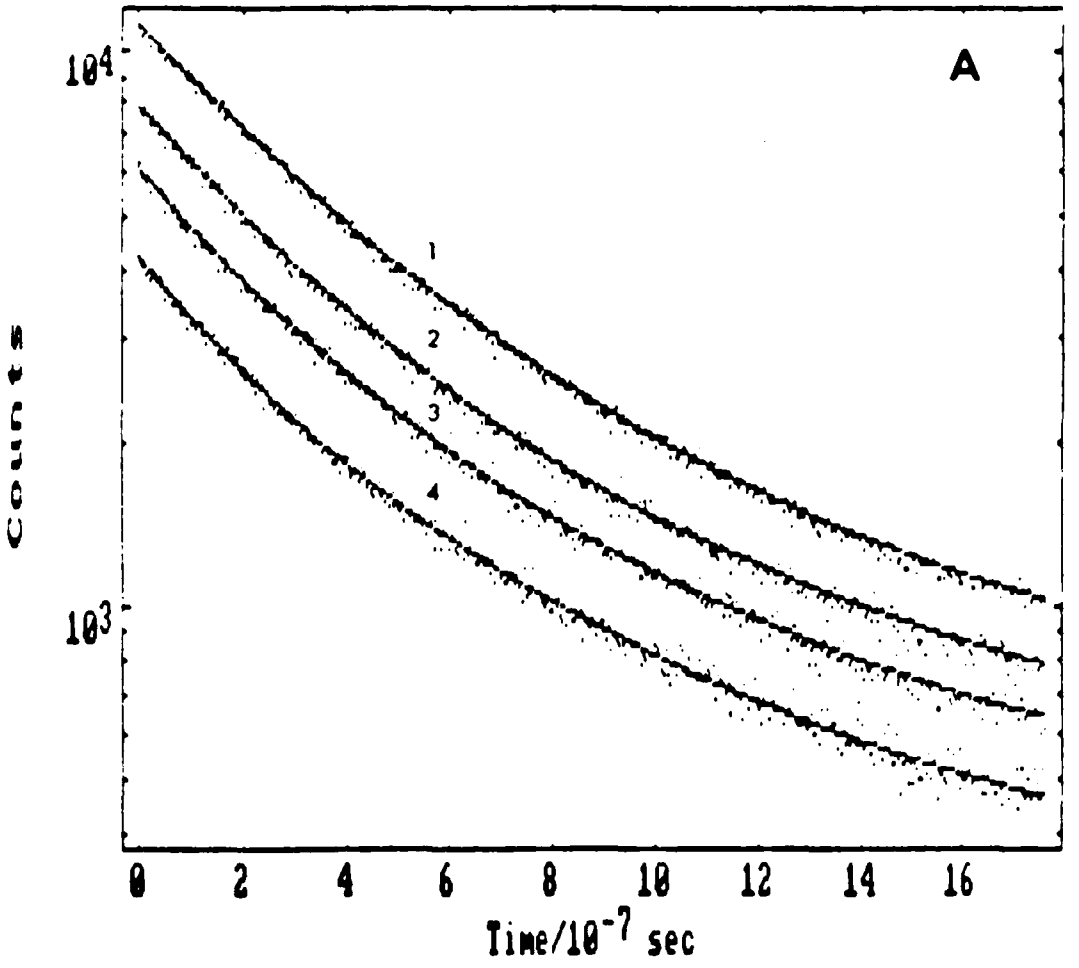
A
10^4
10^3
Counts
1
2
3
4
0
2
4
6
8
10
12
14
16
Time/10^{-7} sec

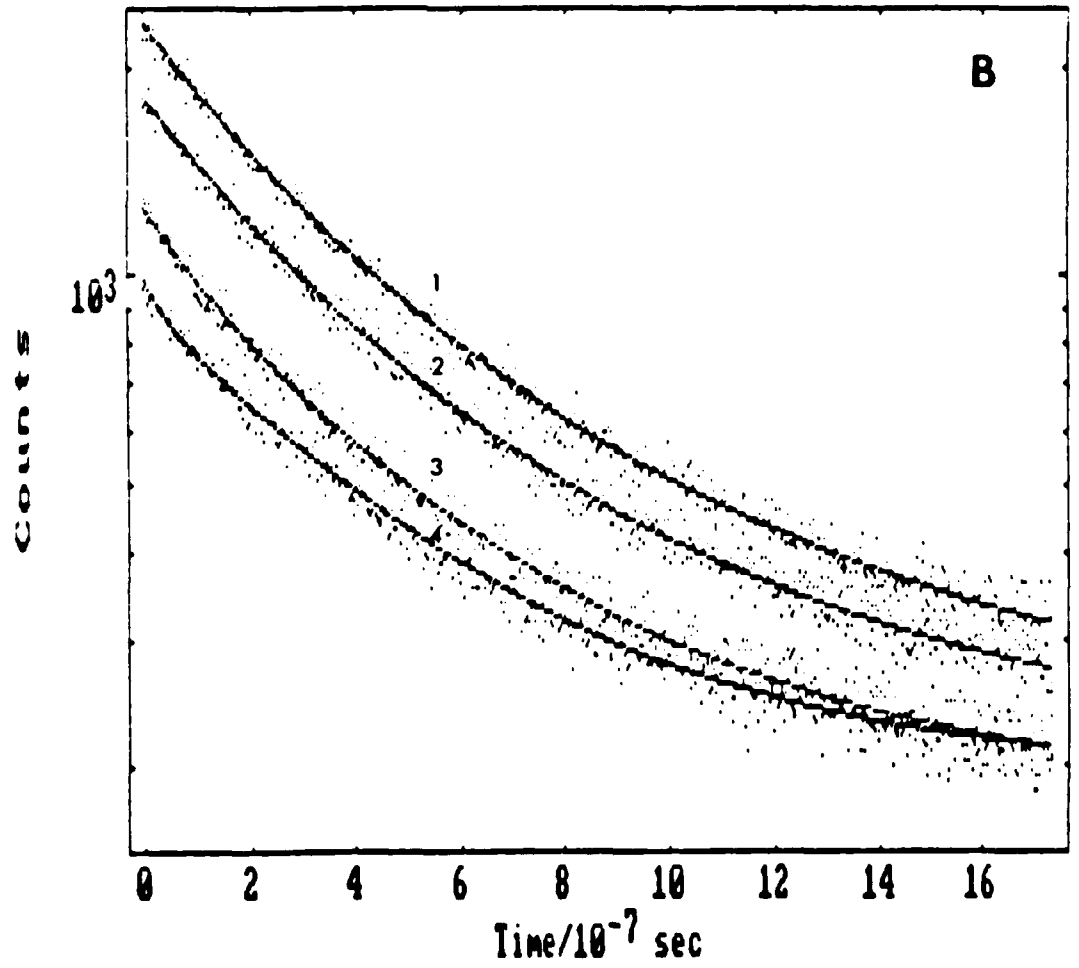
B
10^3
Counts
1
2
3
4
0
2
4
6
8
10
12
14
16
Time/10^{-7} sec

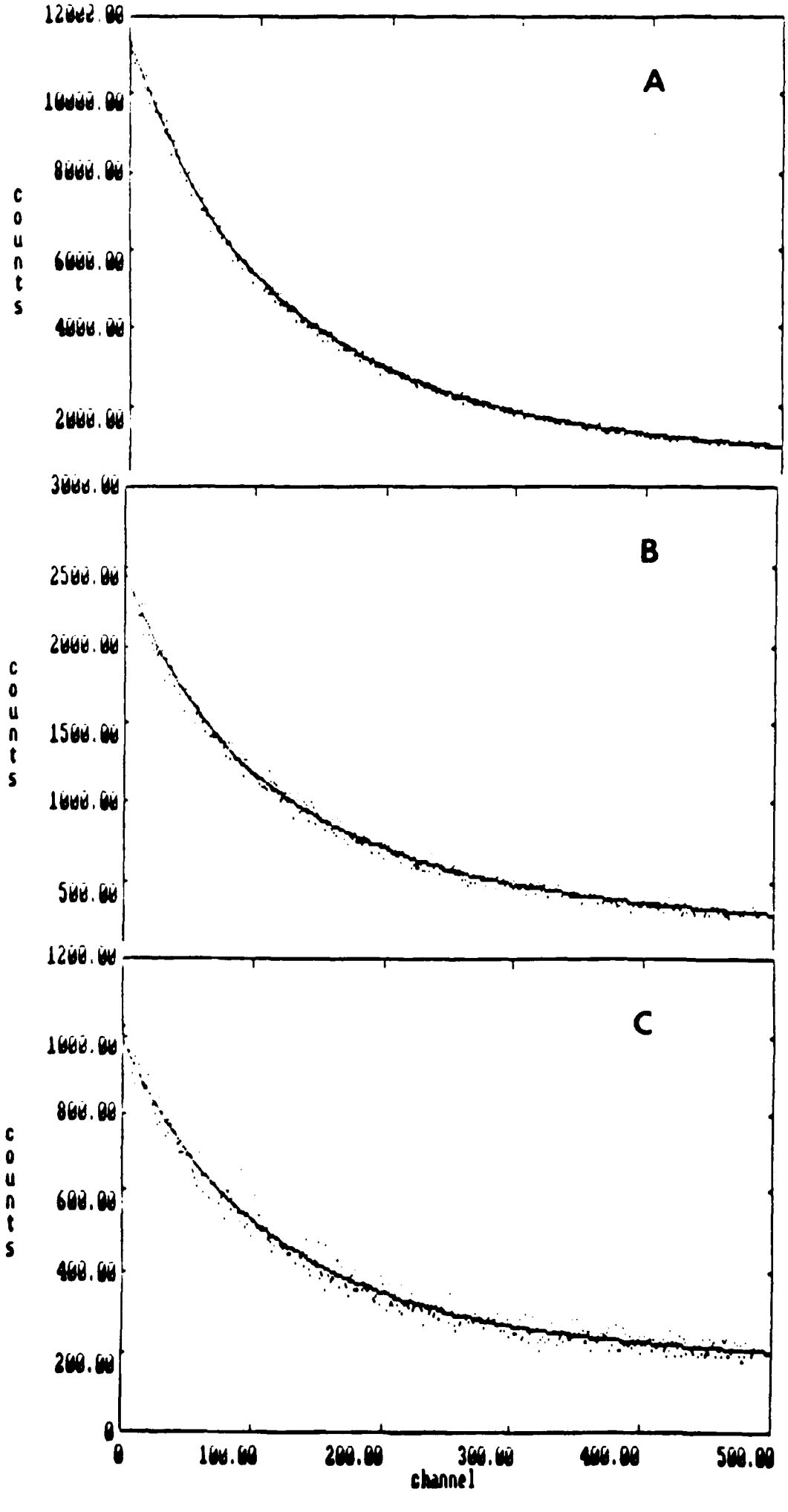
A
B
C
counts
channel
0
100.00
200.00
300.00
400.00
500.00

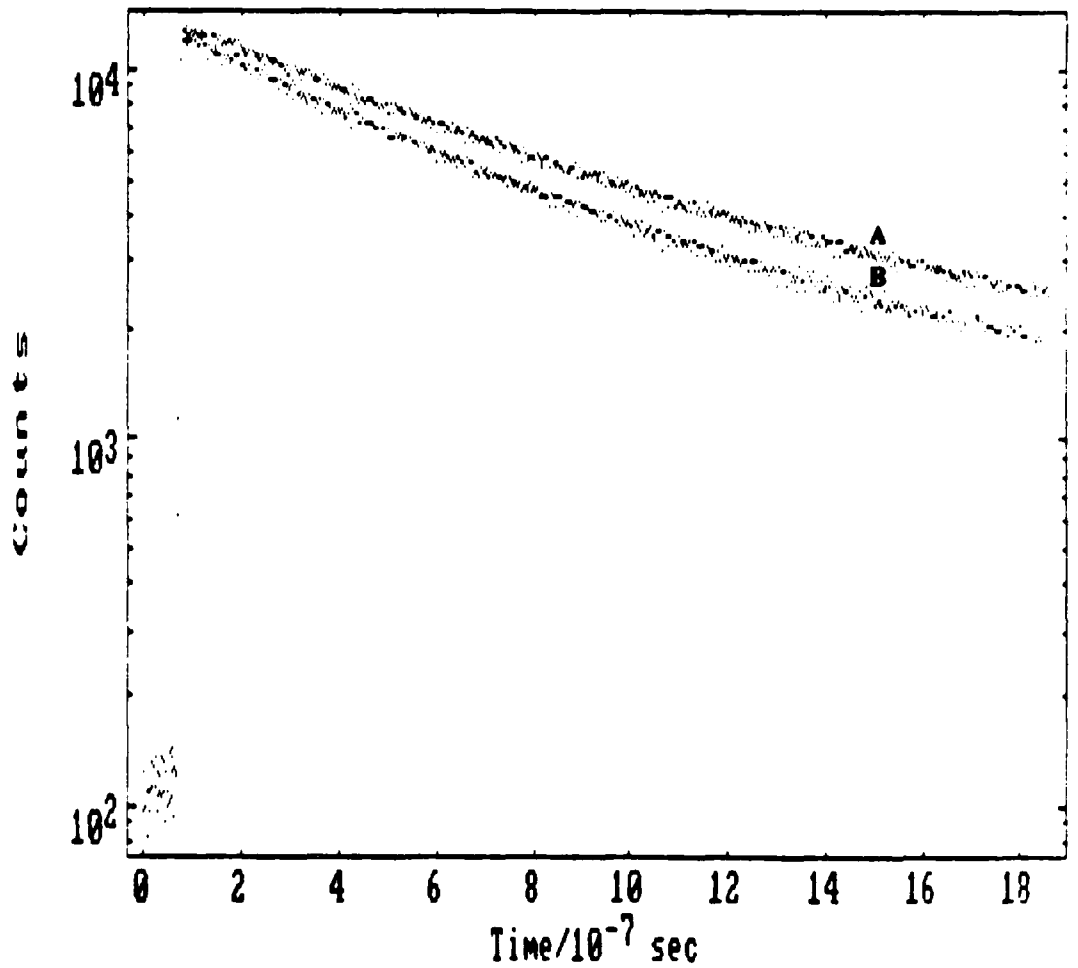
Counts
10^4
10^3
10^2
A
B
0
2
4
6
8
10
12
14
16
18
Time/10^{-7} sec

APPENDIX

DERIVATION OF ALBERY'S EQUATION

The Arrhenius expression for the rate constant is

$$k = Ae^{-Ea/RT}, \tag{A.1}$$

where E_a is the activation energy and A is the preexponential factor. Solving for E_a gives

$$E_a = -RT\ln k + RT\ln A \tag{A.2}$$

Assume a distribution of the energies of activation, the difference between an individual energy of activation (E_{ai}) and the average energy of activation ($\bar{E}_a$) is:

$$E_{ai} - \bar{E}_a = -RT\ln k_i + RT\ln A - (-RT\ln \bar{k} + RT\ln A) \tag{A.3}$$

$$(E_{ai} - \bar{E}_a)/RT = -(\ln k - \ln \bar{k}) \tag{A.4}$$

Now, assume that the energies of activation are distributed in a Gaussian fashion. Each individual energy of activation can be expressed as a function of the average energy of activation and the standard deviation of the distribution, γ

$$(E_{ai} - \bar{E}_a)/RT = -(\gamma x) \tag{A.5}$$

where x is a scaling factor ($-\infty < x < +\infty$). From Equations A.4 and A.5 we obtain

$$(\gamma x) = (\ln k_i - \ln \bar{k}) \qquad (A.6)$$

$$k_i = \bar{k} e^{\gamma x} \qquad (A.7)$$

Equation A.7 will be used later below.

Equation A.5 relates each individual energy of activation to the average energy of activation and γ. We can rearrange equation A.5 to give

$$x = (\bar{E}_a - E_{ai})/\gamma RT \qquad (A.8)$$

Now let us assume that at time zero we have this Gaussian distribution of species where each member of the distribution decays with first order kinetics. The total concentration of these species at time zero ($C_x(0)$) is given by:

$$C_x(0) = \bar{C}(0)\exp(-x^2) \qquad (A.9)$$

Equation A.9 describes a Gaussian where $\bar{C}(0)$ is the middle of the distribution and x the parameter that describes the distribution. The first order rate constant for all the species with a particular x value is given by equation A.7, where $\bar{k}$ is the value at the middle of the distribution. To obtain the equation describing the decay for the whole population of species, having all possible x values, we must start with just one value of x,

and describe the first order kinetics.

The decay law for species corresponding to a single value of x follows the development of the standard first-order decay law

$$dC_x/dt = -k_x C_x \qquad (A.10)$$

substituting the value of k_x from equation A.7 we obtain:

$$dC_x/dt = -C_x \bar{k} e^{\gamma x} \qquad (A.11)$$

We define now a dimensionless time $\tau = \bar{k}t$ and then $dt = d\tau/\bar{k}$. Equation A.11 becomes

$$dC_x/(d\tau/\bar{k}) = -C_x \bar{k} e^{\gamma x} \qquad (A.12)$$

Therefore

$$dC_x/C_x = -e^{\gamma x}\, d\tau \qquad (A.13)$$

Integrating the lhs of equation A.13 from $C_x(0)$ to $C_x(\tau)$ and the rhs from $\tau = 0$ to τ to we obtain

$$\ln(C_x(\tau)/C_x(0)) = -\tau e^{\gamma x} \qquad (A.14)$$

and

$$Cx(\tau) = Cx(0)\exp(-\tau e^{\gamma x}) \qquad (A.15)$$

which gives the concentration of species, having one specific value of x (i.e. one value of E_a), left at time τ. To obtain the total concentration of species left at time τ we must integrate

over all possible values of x

$$C(\tau) = \int_{-\infty}^{+\infty} C_X(\tau)\ dx = \int_{-\infty}^{+\infty} C_x(0)\exp(-\tau e^{\gamma x})\ dx \qquad (A.16)$$

We know that $C_x(0) = \bar{C}(0)\exp(-x^2)$ (equation A.9) and therefore

$$C(\tau) = \int_{-\infty}^{+\infty} C_X(\tau)\ dx = \bar{C}(0) \int_{-\infty}^{+\infty} \exp(-x^2)\ \exp(-\tau e^{\gamma x})\ dx \qquad (A.17)$$

$C(\tau)$ is the total concentration of species left after time τ. Rearranging

$$C(\tau)/\bar{C}(0) = \int_{-\infty}^{+\infty} \exp(-x^2)\ \exp(-\tau e^{\gamma x})\ dx \qquad (A.18)$$

The total concentration of species at time = 0 is

$$C(0) = \int_{-\infty}^{+\infty} C_X(0)\ dx \qquad (A.19)$$

and substituting the distribution function of equation A.9 in equation A.19 we obtain

$$C(0) = \bar{C}(0) \int_{-\infty}^{+\infty} \exp(-x^2)\ dx \qquad (A.20)$$

Rearranging

$$\bar{C}(0) = \frac{C(0)}{\int_{-\infty}^{+\infty} \exp(-x^2)\ dx} \qquad (A.21)$$

Using equation A.21 we have that

$$C(\tau)/\bar{C}(0) = [C(\tau)/C(0)] \int_{-\infty}^{+\infty} \exp(-x^2)\, dx \qquad (A.22)$$

and

$$C(\tau)/C(0) = \frac{C(\tau)/\bar{C}(0)}{\int_{-\infty}^{+\infty} \exp(-x^2)\, dx} \qquad (A.23)$$

Substituting equation A.18 in the numerator of equation A.23 we obtain Albery's equation:

$$C/C_o = \frac{\int_{-\infty}^{+\infty} \exp(-x^2)\, \exp[-\tau\, \exp(\gamma x)]\, dx}{\int_{-\infty}^{+\infty} \exp(-x^2)\, dx} \qquad (A.24)$$

where $$\int_{-\infty}^{+\infty} \exp(-x^2)\, dx = \pi^{1/2}$$

Note that by assuming a Gaussian distribution in ln k only two adjustable parameters are needed to describe the distribution: $\bar{k}$, the rate constant of maximum probability, and γ, the measure of the width of this distribution. As noted in the experimental section, these parameters were obtained by fitting simulated and experimental transients.